

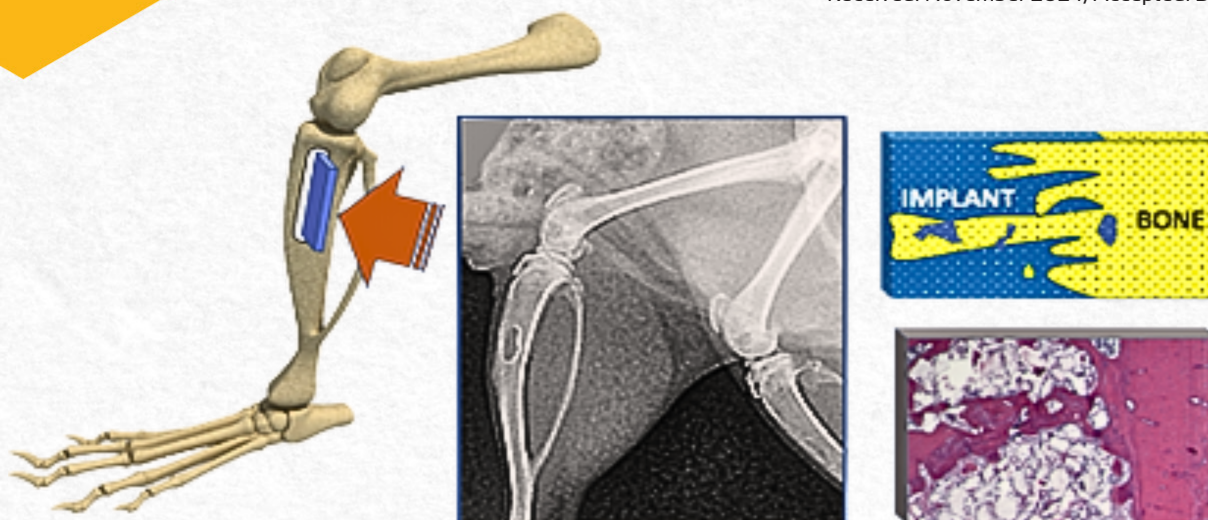


Enhanced bone implant with porous polypropylene matrix coated with chitosan and hydroxyapatite

J. I. Arias¹; A. Neira-Carrillo²; M. Yazdani-Pedram³

*Corresponding author: E-mail address: iaras@uchile.cl

Received: November 2024; Accepted: December 2024.



Statement of significance

This study shows successful osteointegration and osteoconduction of a novel porous grafted polypropylene coated with chitosan and hydroxyapatite composite in rat tibial defects, resulting in an apparently anchored bone implant. Such information should be particularly useful in the design of biocompatible bone implants or scaffolds, especially in minimally loaded conditions where an effective bone implant anchorage is required.

Abstract: Porous polymer matrix based on functionalized polypropylene coated with chitosan and hydroxyapatite was prepared to evaluate its body response and establish its ability to induce osteointegration and/or osteoconduction. 12 Sprague-Dawley rats were divided into 6 groups corresponding to 0, 1, 2, 4, 8 and 16 weeks of healing; a 5x1 mm bone defect was created in the proximal diaphysis of both tibiae. In the right member the composite to evaluate was introduced and the left member was used as control. Animals were sacrificed by CO₂ chamber and a radiographic and histological study was done. The implanted composite showed no evidence of foreign body reaction from the first week and maintained close contact with newly formed bone tissue. During the first two weeks a periosteal reaction penetrating the implant pores was observed. Osteogenic buds observed as mesenchymal cells condensations highly vascularized and newly trabecular bone formations were found within the implant pores. New bone formation was observed until the eighth week after implantation when morpho-structural adaptation began. We concluded this matrix coated with chitosan and hydroxyapatite exhibited osteointegrated properties because it's structurally binding to bone and osteoconductive properties due to adhesion, proliferation, and differentiation of the osteoblastic cells within their pores.

Keywords: Grafted polypropylene. Chitosan hydroxyapatite coating. Bone implant.

¹Regenerative Medicine Lab (Bimre), Faculty of Veterinary and Animal Science, University of Chile

²Polyforms Lab, Faculty of Veterinary and Animal Science, University of Chile

³Department of Organic Chemistry, Faculty of Chemical and Pharmaceutical Sciences, University of Chile

Introduction

Bone tissue is the main component of the skeleton and is a tissue with a strong capacity for regeneration after a trauma, forming new bone identical to the pre-existing tissue^{1, 2}. The need to restore various types of bone defects has long been an important area of research in medical science³.

As has been well studied and reviewed, when bone is injured, several mechanisms are triggered to heal and remodel the damaged tissue⁴. However, if the defect is too extensive (more than 6 mm) or too unstable, the healing mechanisms may fail or be delayed resulting in the formation of a nonfunctional fibrocartilage callus and permanent bone nonunion. In some of these cases, especially when the bone architecture must be preserved, bone grafting or implant replacement is recommended⁵.

Currently, rather than using permanent prosthetic implants to replace damaged tissues, the ultimate goal of surgery is to implant temporary reconstructive scaffolds that allow and promote self-regeneration⁶.

Bone is a complex dynamic tissue, in constant formation and resorption. It is a natural hierarchical structured biocomposite consisting mainly of a collagen matrix reinforced with hydroxyapatite (HA) and cells⁷, such as osteocytes in combination with osteoclasts, which together are capable of controlling bone remodeling by sensing mechanical load variations⁸.

Bone remodeling is a physiological and constant process involving the resorption of a certain amount of bone carried out by osteoclasts, which secrete lysosomal enzymes that demineralize and degrade bone matrix, and osteoblasts, which secrete and mineralize new osteoid matrix⁶.

Bone regeneration after injury involves blood vessels, cells, and extracellular matrix interactions. After trauma, initial hematoma and inflammatory responses occur. Clot cells release growth factors and interleukins that induce the migration of lymphocytes, macrophages, osteoclast precursors, and pluripotent mesenchymal stem cells to the injured site. Additionally, these molecular signals also promote the differentiation of endothelial cells, fibroblasts, chondroblasts, and osteoblasts, generating new fibrovascular tissue that eventually replaces the initial clot⁸⁻¹⁰.

Ongoing efforts are being made for the development of different materials suitable for use as bone supports that have special properties such as osteoinduction, osteoconduction, and osteointegration^{8, 11}. Osteoinduction is the ability to stimulate pluripotential mesenchymal stem cells to proliferate and differentiate^{8, 11}. Osteoconduction is the ability to stimulate adherence and migration

of osteogenic cells and blood vessels and colonization of bone cells inside the porous implant. Osteointegration corresponds to the structural and functional direct connection between bone and the implant^{8, 11}. Previous studies have shown that osteointegration of biomaterials depends on support properties, such as surface loading, topography, and appropriate porosity¹².

The newest polymeric bioimplantable materials for bone healing need to create supports comprising complex structural and macroscopic forms that allow multiple options to accommodate different bone tissue structures¹³. These bioimplantable supports must also have a highly interconnected, over 90% porous microstructure and a large conducting surface area for the development of new tissue ingrowth. For bone regeneration, the porosity should vary between 100 and 350 μm ¹⁴. These supports or composite materials act as substrates for adhesion, proliferation, and differentiation of cells^{12, 14, 15}. They have been modeled from biodegradable materials of natural origin (such as collagen or hyaluronic acid), synthetic polymers (such as peptide amphiphilic materials¹⁶, including poly (3-hydroxybutyric acid)-co-(3-hydroxyvaleric acid), poly (glycolic acid), poly (lactic- acid), polypropylene-carbonate), and natural bone substitutes (such as eggshell¹⁷⁻¹⁹ hydroxyapatite and hydroxyapatite / collagen / chitosan composite scaffolds, which turned out to be highly biodegradable and biocompatible¹⁴. HA can be obtained synthetically and possesses good biocompatibility, non-toxic activity, chemical stability, osteoconduction characteristics, and bioactive properties. Although its resistance to tensile forces is low, its micropores favor the progressive tendency to reabsorption and subsequent substitution by host bone^{20, 21}. HA has also been used in combination with chitosan (CH), a natural cationic polysaccharide which can be produced by N-deacetylation of chitin. Important properties of this polymer, such as biocompatibility, chemical resistance, mechanical strength, antimicrobial properties, and thermal stability, have stimulated its use in biotechnology²²⁻²⁴.

On the other hand, non-biodegradable biomaterials like polyester- and polyfumarate-based polymeric supports, high density polyethylene microspheres, or polypropylene (PP)-based implants whose porosity allows rapid growth of fibrovascular tissue and ultimately bone reconstruction have been widely used as bone scaffolds in low load-bearing applications²⁵.

PP is a polyolefin synthesized via catalysis from propene and has been recently studied as a biomaterial composite²⁶⁻²⁸. It has been well established that PP or PP-oxide does not demonstrate good biocompatibility, showing a lack of contact with fibrous or

bone tissue²⁹⁻³¹. Bone scaffolds composed of PP biocomposites reinforced with HA^{32,33} or carbon nanotubes²⁶ have been tested for cell viability in vitro, and PP + CH used in vivo in a rabbit bone defect model showed a faster osteogenesis rate than PP-alone³⁴. Additionally, PP functionalized with CH improves in vitro fibroblast adhesion and proliferation³⁵. When polyethylene/hydroxyapatite nanocomposites were used, it was shown that a strong and stable interface was developed between the composites and the host bone³⁶. However, no implants have yet been tested in vivo to exploit the advantages of CH and HA when used in combination with porous grafted PP.

Here, we tested for the first time in vivo, implants based on porous polypropylene grafted with monomethylitaconate coated with CH and HA in rat tibial bone defects to analyze their osteointegrative and osteoconductive properties.

Materials and methods

Porous grafted polypropylene (PGPP) scaffolds

A previously reported method was used to prepare the PGPP²⁸. Briefly, 5 g of PP grafted with 0.7% monomethylitaconate was dissolved in 100 ml of xylene at 110 °C in a water bath with constant stirring. Then the grafted PP was precipitated with cold methanol, filtered, and washed with abundant water and acetone. The precipitated grafted PP

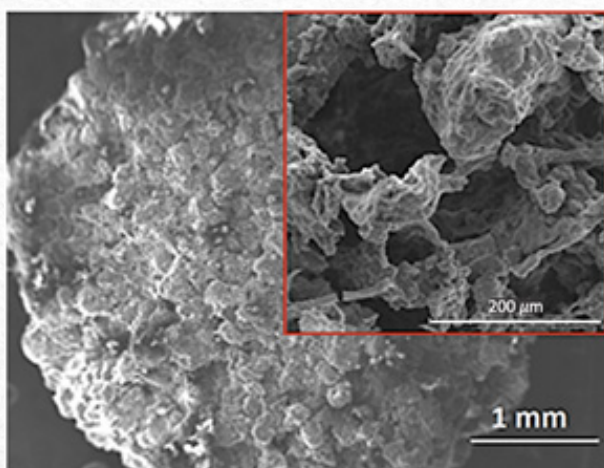


Fig. 1. SEM images of PGPP-CHHA composite before being implanted in rat tibial defect showing rough surface and irregular interconnected pores, 50 to 250 μm in size.

were dried in a vacuum oven at 60 °C for 3 days. Powdered grafted PP were obtained by grinding in a cryogenic mill at 5 °C for 5 min and the particles were sieved in the range of 150 to 300 μm . These particles were molded in a metallic mold using 1 g of grafted PP and 40 mg of NaHCO₃ as blowing agent, and the mold was placed in a furnace at 190 °C for 30 min and then rapidly immersed into cold water to detach the porous scaffold.

The PGPP obtained was coated with CH and HA (PGPP-CHHA) by immersion in 1% CH, Mw=70 kDa, >75% deacetylation (Aldrich and Fluka[®]) in 2% acetic acid with 0.5% commercial HA (Sigma Aldrich[®]) for 21 days. The PGPP-CHHA was dried at room temperature, sectioned, and sterilized with ethylene oxide for 24 hours in individual sachets. The surface morphology and pore size of the PGPP-CHHA were examined using a TESLA BS 343A scanning electron microscope (SEM) operating at 15 kV. The specimens were coated with a 20-nm thick gold layer using an EMS-550 automated sputter-coater with the current set at 25 mA for 4 min (Fig. 1). Histological cross-section of the PGPP-CHHA implant before in vivo implantation showing pores (p) cross-section. H (red) and HA spicule crystals (blue) localized inside the interconnected-pores (Fig. 2).

Experimental animals and surgery

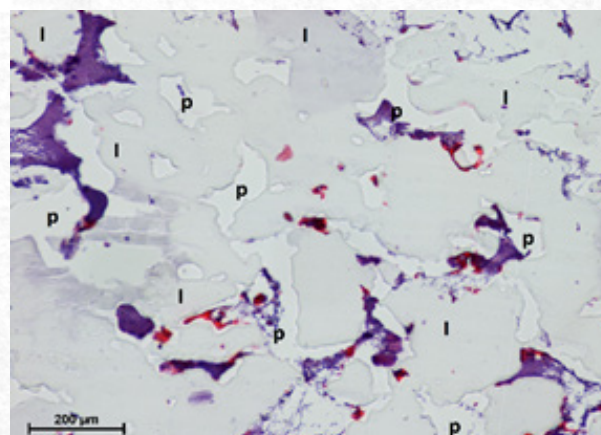


Fig. 2. Histological cross-section of the PGPP-CHHA implant (i) before in vivo implantation showing pores (p) cross-section. CH (red) and HA spicule crystals (blue) localized inside the pores. Hematoxylin-eosin, 10x.

All animal procedures were approved by the Institutional Animal Bioethics Committee, and the animals used in this study received humane care in accordance with the Guide for the Care and Use of Laboratory Animals prepared by the National Academy of Sciences and published by the National Institutes of Health (NIH publication No. 85-23, revised 1985).

According to the ISO 10993 norm, for the biological evaluation of biomaterials as medical devices, 12 female Sprague-Dawley rats 10-12 weeks' old were used. Animals were divided into 6 groups corresponding to 0, 1, 2, 4, 8, and 16 weeks of healing. Rats were housed in separate cages and fed commercial pellets and water ad libitum.

Surgery and composite implantation: Working under an isoflurane inhalation anesthesia protocol by mask and open circuit, both hind limbs were shaved from the proximal third of the femur to the distal third of the tibia. Disinfection was accomplished with 0.5% chlorhexidine and ethanol to proceed with a longitudinal incision of the skin at the tibial crest followed by debridement of the cranio-medial musculature of the tibia and

periosteum. Then a rectangular defect of the medial cortical bone subjacent to the tibial crest was created to reach the medullary canal in both legs of each rat (Fig. 3).

The defect, approximately 5 mm long and 1 mm wide, was made with a manual electric drill using a 1-mm diameter drill bit. In each animal the right tibia was considered as experimental and the left tibia as positive control. In the cortical defect of the experimental group, the composite was introduced by digital pressure, and then the separated tissues were sutured with 4/0 absorbable polyglycolic acid suture with a simple discontinuous suture pattern. The tibiae of the positive control group were subjected to the same procedure but without the introduction of the composite in the cortical defect. After these procedures, treatment was administered subcutaneously: Ketoprofen 1 mg / kg every 24 hours for 3 days as an anti-inflammatory and antibiotic enrofloxacin every 24 hours for 7 days. Each group was evaluated at weeks 0, 1, 2, 4, 8, and 16 post-implantations. Rats were sacrificed in a carbon dioxide (CO₂)-saturated chamber

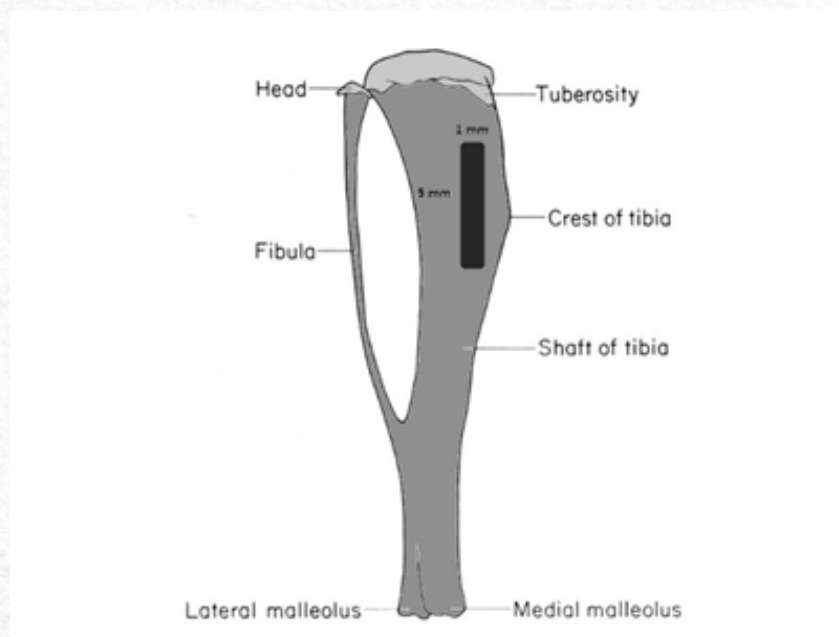


Fig. 3. Diagram of the lower leg bone showing the 5 x 1-mm defect done surgically in the tibial tuberosity.

Histological evaluation

Experimental and control tibiae were extracted and fixed in 10% formalin for 5 days; washed in water and decalcified in Ana Morse solution 37 for 14 days, with the solution changed daily. Then samples were processed for routine histological fixation, embedding, and cutting into 0.5- μ m thickness crestal tibial cross sections stained with hematoxylin-eosin (H&E). Sections were analyzed in an optic microscope (Nikon Eclipse E-600) taking digital pictures at 4x, 10x, and 40x with 2560 x 1920-pixel resolution with a digital video camera (Cool Snap-Pro CF, Media Cybernetic, USA) using a morphometric software (Image Pro-Plus, Media Cybernetics, USA).

Radiographic assessment

Orthogonal radiographic views of the tibia were taken from the 12 post-mortem rats to determine the degree of periosteal reaction, soft tissue reaction, and bone radiodensity at the site of the lesion as indicative of bone callus formation. Radiographs were photographed with a digital camera. Images were scored for the degree of periosteal and soft tissue reaction as Null (N), mild (+), moderate (++), and strong (+++)

Results

SEM study

The study showed measurements of pore sizes of the scaffolds, as determined by Scanning Electron Microscopy (SEM), range between 50 to 250 μ m²⁸. This pore size range is critical as it supports cellular attachment, proliferation, and vascularization, which are essential for effective bone regeneration. These highlights that the scaffolds showed a lower percentage of grafting (specifically 0.7%-0.9% of MMI) and demonstrated a well-interconnected porous structure, making them suitable for in vivo studies.

Radiographic study

At time 0 in both tibial injuries, no new bone formation was observed. However, a radiolucent defect, measuring 5 x 2-mm with clear margins was visible (Fig. 4a). After one week, the control tibia showed mild periosteal and soft tissue reaction, while the treated tibia showed no periosteal or soft tissue reaction (Fig. 4b). After two weeks, the control tibia exhibited moderate periosteal and mild soft tissue reaction with a 4 x 1-mm injury, while the treated tibia showed mild periosteal or moderate soft tissue reaction, but no change in the size of the injury (Fig. 4c). After four weeks, the control tibia exhibited no periosteal and mild soft tissue reaction, with a 2 x 0.5-mm injury. In contrast, the treated tibia showed moderate periosteal and soft tissue

reaction, but no change in the size of the injury (Fig. 4d). At eight weeks post-surgery, the control tibia showed no periosteal or soft tissue reaction, and no observable injury. However, the treated tibia exhibited strong periosteal or moderate soft tissue reaction, and the injury site was still observable (Fig. 4e). After sixteen weeks from the creation of the original defect, there was no periosteal and soft tissue reaction in both the control and the treated tibiae. However, the treated tibia showed a smaller injury site of 2 x 1-mm, while no injury site was found in the control there (Fig. 4f). Table 1 summarizes the radiological observations made throughout the experiment in terms of periosteal and soft tissue reaction.

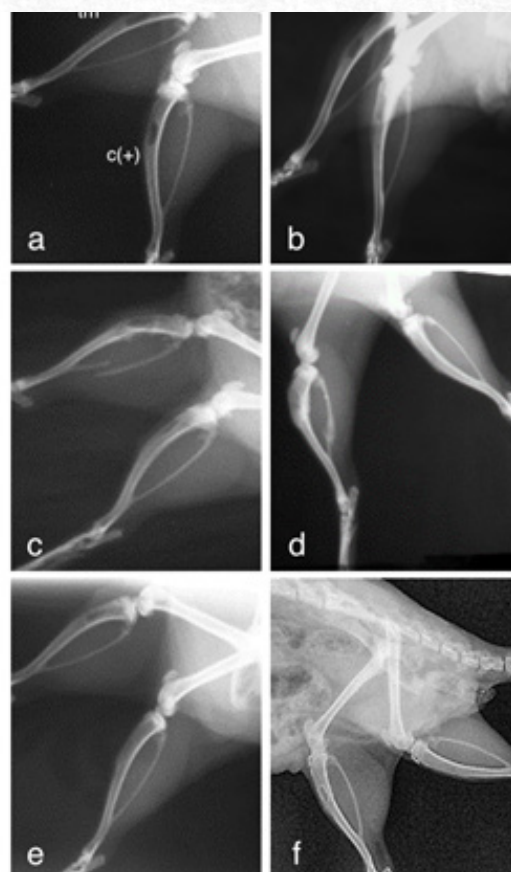


Fig. 4. Orthogonal radiographic images of treated (tm) and control (C+) rat tibiae show the progression of the tibial bone defect over time: at time zero (a), 1 week (b), 2 weeks (c), 4 weeks (d), 8 weeks (e), and 16 weeks (f). It is worth noting that defect size in the control tibia is not observable at 8 weeks, while in the treated tibia it remains visible until the last week of the study, albeit smaller than the original defect.

Table 1. Radiographic image description as degree of periosteal and soft tissue reaction.

	WEEKS											
	0		1		2		4		8		16	
	Exp*	Cont	Exp	Cont								
Periosteal	N**	N	N	+	+	++	++	N	+++	N	N	N
Soft tissue	N	N	N	+	++	+	++	+	++	N	N	N

* Exp = Experimental; Cont = Control
 ** Null (N); Mild (+); Moderate (++); Severe (+++)

Histological study

In the positive control treatments, an inflammatory phase was observed during the first week after the bone lesion. This phase was characterized by the formation of a blood clot and the infiltration of abundant blood vessels, inflammatory cells, and fibroblasts (Fig. 5a and Fig. 5b). By the second week, the site of the injury was covered by periosteal tissue and immature trabecular woven bone filled

the medullary canal and partially bridges the injured cortical bone (Fig. 5c). Between the second and fourth week, the bone bridge of the cortical bone thickens and matures (Fig. 5d). By the eighth week, the woven bone of the medullary canal progressively diminishes, while the bone marrow appears more abundant (Fig. 5e). Sixteen weeks after the injury, a complete healing of the bone structure was observed (Fig. 5f).

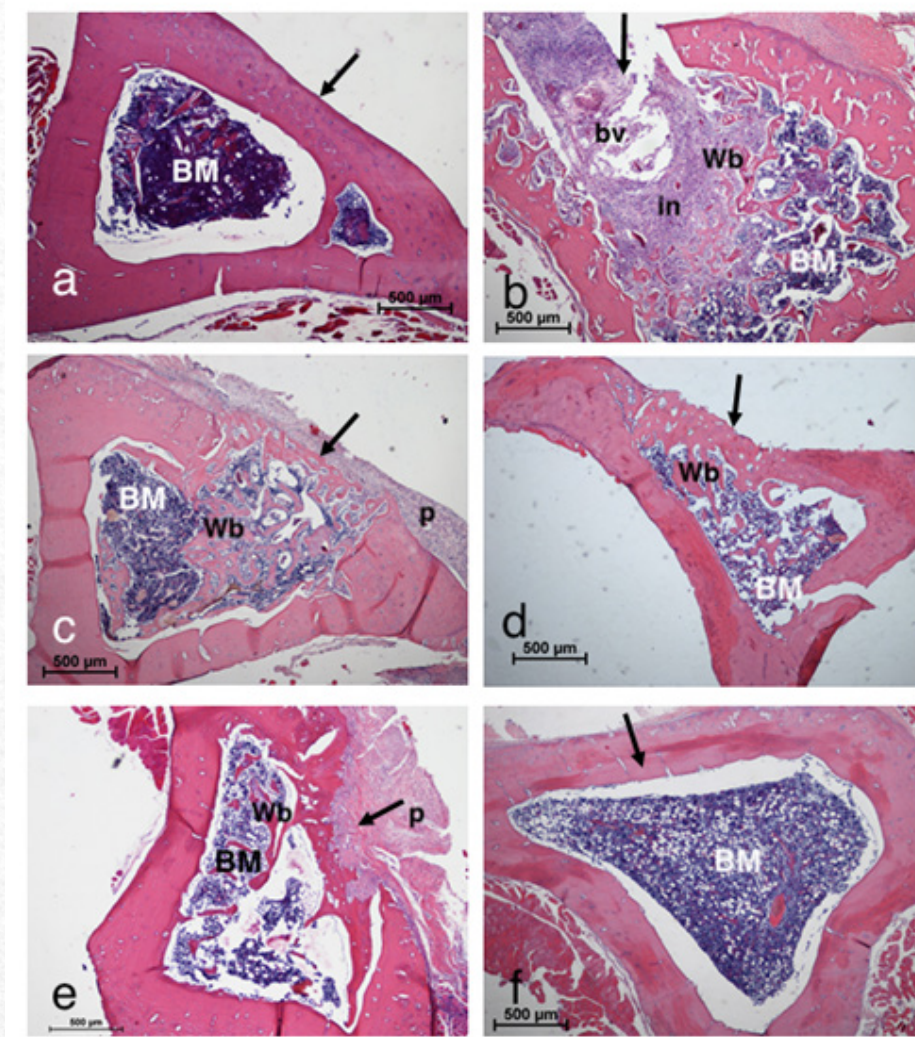


Fig. 5. Microscopic images of positive control tibiae cross sections stained with H&E, at time zero (a), 1 week (b), 2 weeks (c), 4 weeks (d), 8 weeks (e), and 16 weeks (f). Bone defect area (arrow), woven bone (wb), bone marrow (BM), and periosteum (p) are indicated. 40x.

In the experimental treatments at time 0, the cortical bone continuity is interrupted, and the composite occupied the surgically produced defect and the bone marrow cavity (Fig. 6a and Fig. 7a). After one week, a moderate endosteal activity was observed, which can be seen as the invasion of a few cells around the composite matrix and inside its pores. In addition, abundant cells forming osteogenic buds and some new woven bone formation with immature bone trabeculae were observed adjacent to the cortical bone (Fig. 6b and Fig. 7b). After two weeks of implantation, there was increased endosteal activity both around and inside the polymeric implant, as well as in the invasion of the pores. Trabecular new bone formation and

cortical bone resorption were also observed (Fig. 6c and Fig. 7c). By the fourth week, the composite had been surrounded and invaded by endosteum, with the pores filled. Osteogenic buds and small blood vessels were also observed inside the pores (Fig. 6d and Fig. 7d). At eight weeks post-implantation, the small pores of the implant were full of endosteal cells, and there were abundant osteogenic buds and small vessels. Woven bone trabeculae were observed crossing through the large pores of the composite (Fig. 6e and Fig. 7e). By the sixteenth week, abundant trabecular bone was observed inside the larger pores of the implant together with osteoid anchoring the PP-matrix (Fig. 6f and Fig. 7f).

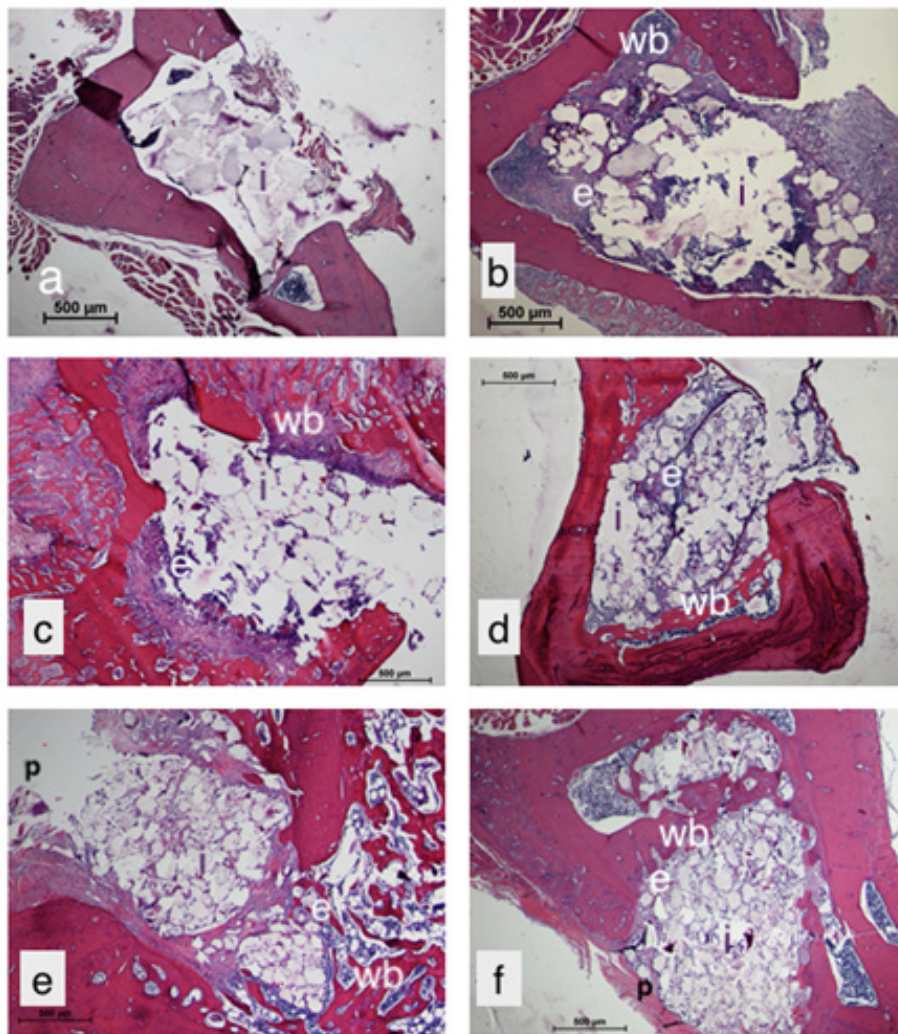


Fig. 6. Microscopic images (40x) of cross sections stained with H&E of treated tibiae with coated PP implants at time zero (a), 1 week (b), 2 weeks (c), 4 weeks (d), 8 weeks (e), and 16 weeks (f). Woven bone (wb), endosteum (e), PP implant (i), and periosteum (p) are indicated.

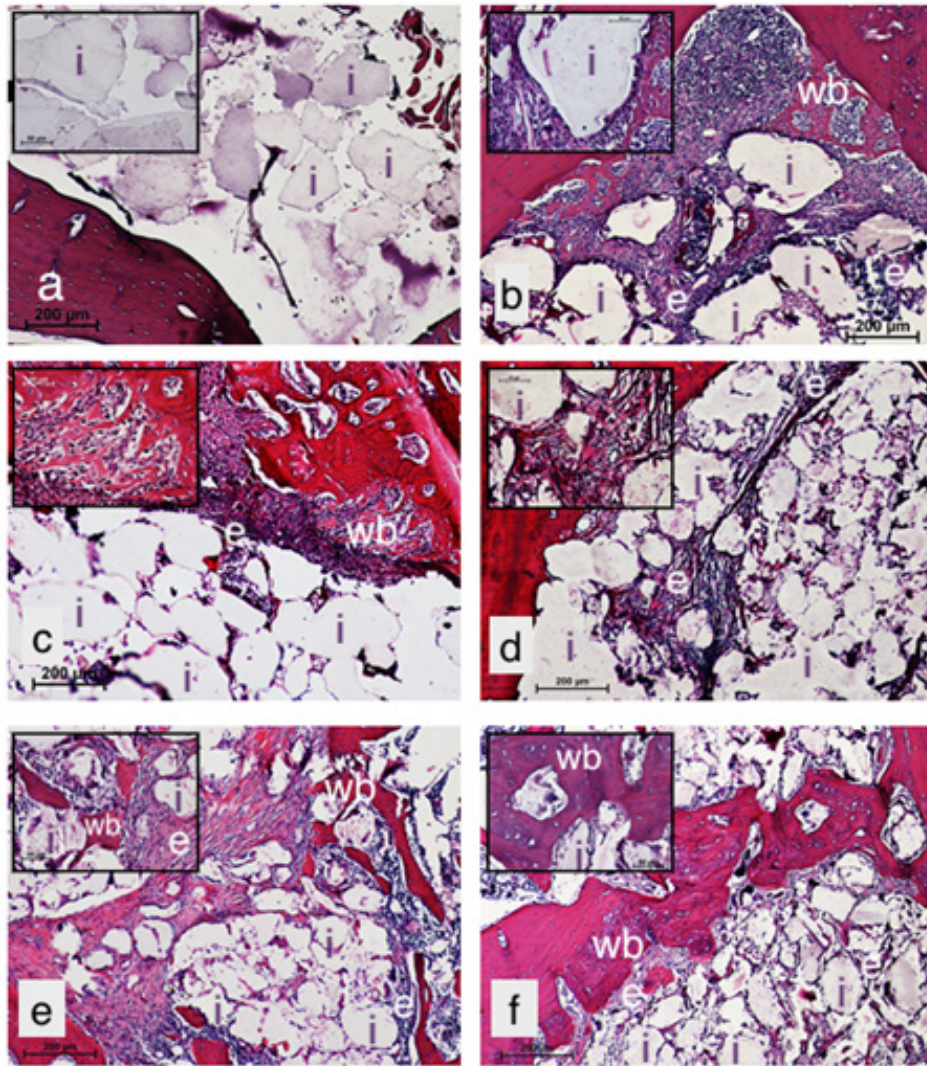


Fig. 7. Microscopic images (100x and 400x (inset)) of cross sections stained with H&E of treated tibiae with coated polypropylene composite implants at time zero (a), 1 week (b), 2 weeks (c), 4 weeks (d), 8 weeks (e), and 16 weeks (f). Woven bone (wb), endosteum (e), and PP implant (i) are indicated.

Discussion

It is widely accepted that polypropylene (PP) is a highly stable polyolefin that is non-biodegradable when used in vivo, and allergic reactions to this material are very rare³⁸. However, PP is not suitable for use in the stabilization of bone defects submitted to load-bearing due to its mechanical properties³⁹. When used as a membrane in contact with an unloaded calvarial critical bone defect, it only guides bone regeneration under its surface without osteointegration or adhesion to surrounding bone, acting as an inert material^{29,40}.

Therefore, the relevance of pore size to the success of the osteoconductive properties of biomaterials is a critical factor in bone tissue engineering, especially in the context of using polymer-based scaffolds like the polypropylene grafted with monomethylitaconate (PP-g-MMI). The osteoconductive properties of

biomaterials rely heavily on their ability to support cell attachment, proliferation, and subsequent bone formation within the scaffold structure.

Optimal pore size plays a vital role in facilitating cellular infiltration, nutrient diffusion, vascularization, and bone tissue ingrowth. Studies suggest that pore sizes between 100-300 µm are generally considered ideal for promoting osteogenesis, as they allow for sufficient space for osteoblast attachment and new bone matrix deposition while also enabling vascularization, which is crucial for sustained bone growth and healing⁴¹. Our scaffold features interconnected pores ranging from 50-250 µm, which falls within this optimal range. This pore size supports not only cellular migration but also the formation of new bone, which is essential for the scaffold's integration with the host bone tissue²⁸.

Interestingly, while larger pores are beneficial for

bone ingrowth, they can compromise the mechanical strength of the scaffold. PP-g-MMI scaffolds with smaller pore sizes exhibited higher mechanical properties, such as fracture resistance and reduced deformation. This trade-off between mechanical stability and biological efficacy highlights the need for a balanced pore size that can support both load-bearing and osteoconductive functions⁴².

The use of functionalized polypropylene with polar monomers like monomethylitaconate enhances the scaffold's surface properties, making it more conducive to bone regeneration. These functional groups improve the adhesion of bioactive molecules like hydroxyapatite (HA), promoting mineralization within the scaffold pores. Additionally, the incorporation of chitosan in combination with HA in the PP-g-MMI scaffolds was shown to enhance swelling behavior and the scaffold's capacity to support bone tissue formation, thus demonstrating the importance of both chemical composition and physical structure⁴². Achieving the right pore size is crucial for maximizing the osteoconductive properties of biomaterial scaffolds. The balance between sufficient porosity for biological activity and adequate mechanical strength is key to the successful application of these scaffolds in bone repair and regeneration.

CH has been used as a scaffold or hydrogel for osteochondral tissue engineering because of its chemical similarities with glycosaminoglycans found in bone and cartilage⁴³⁻⁴⁷. It exhibits osteocompatible, osteoconductive, and antimicrobial properties^{48,49}, but has weak biomechanical strength⁵⁰. However, when combined with HA, CH scaffolds show improved mechanical strength, osteoconductivity, and tissue regenerating effectiveness^{51,52}. The review of recent studies shows that HA enhances osteogenic effects CH scaffolds⁵³. Both HA and CH are well-established materials for biological applications⁵⁰. The combination of bioactive inorganic materials, such as HA, tricalcium phosphate and coral calcium carbonate with biocompatible but weak organic degradable or non-biodegradable polymers synergistically improves the desirable properties for application in osteochondral lesions under very low load-bearing conditions⁵³. Biodegradable medical grade polymers, both natural and synthetic, with adjustable degradation rates are available⁵⁵. Nevertheless, they still have some drawbacks such as weak resistance to biomechanical loads^{39,55}, difficulties with intra-operative sculptability, high swelling behavior, and frequent inflammatory responses due to acidic degradation products⁵⁵. In case of relatively large osteochondral lesions with low load-bearing conditions, sculptable three-dimensional porous scaffolds have been used as

supporting structures. For this purpose, the use of synthetic non-biodegradable polyolefin-derived polymers, mainly polyethylene, have been reported⁵⁶. Porous high-density polyethylene has been applied to the fabrication of non-permanent implants for facial and cranial reconstruction, allowing only soft tissue ingrowth⁵⁶.

For bone implants, it is desirable to have permanent implantability and achieve mechanical and biological integration. Once such a bone implant is well integrated, it is less likely for a patient to experience infections, undesirable immune responses, or implant mechanical failure⁵⁷. Therefore, bone implants must be designed to stimulate host tissue functions and provide a suitable microenvironment for the proliferation and differentiation of host cells and the reconstruction of new healthy bone.

Pore size plays an important part in this implantability. Pore sizes above 50 μm are generally recognized as sufficient to facilitate cellular attachment and migration, which are the primary steps in osteoconduction⁴¹. Smaller pores may hinder cell migration, while excessively large pores can compromise mechanical stability. The scaffolds in this study, with their interconnected porous structure, provide a balance between these parameters, promoting adhesion of osteogenic cells and enhancing their proliferation.

The optimal pore size for cell proliferation and osteoid deposition is typically reported to be between 100 and 200 μm ⁵⁸. This is because pores in this range provide adequate space for extracellular matrix (ECM) deposition, critical for forming new bone. The scaffolds' pores within this range likely encourage osteoblast proliferation and the formation of a mineralized matrix, facilitating successful integration with the host bone.

On the other hand, vascularization, a critical factor in osteoconduction, is enhanced in scaffolds with pore sizes exceeding 100 μm ⁵⁹. The upper range of 250 μm observed in this study supports the formation of microvascular networks, which ensure nutrient and oxygen diffusion throughout the scaffold. This interconnected porous structure enables sustained cellular activity and prevents hypoxia, contributing to the long-term success of the biomaterial.

The interconnected porous structure observed in these scaffolds is vital for osteoconduction as it ensures the continuous migration of cells and diffusion of nutrients. Previous studies have demonstrated that scaffolds with well-interconnected pores significantly improve in vivo bone regeneration outcomes due to enhanced vascular infiltration and cell ingrowth⁶⁰.

The interconnected pores ranged from 50-250 μm in these implants, which falls within this optimal

range. This pore size supports not only cellular migration but also the formation of new bone, which is essential for the scaffold's integration with the host bone tissue²⁸. This is seen in our histological results, by the fourth week, where osteogenic buds and small blood vessels are observed inside the pores.

When a bone lesion is created experimentally, as reported here, the bone undergoes the normal stages of the bone fracture healing process^{4, 61}. An initial transitory radiological soft tissue reaction occurs. However, when porous grafted polypropylene embedded with chitosan / hydroxyapatite is implanted into the injured tibia, a radiological soft tissue reaction, as observed here, indicates continued activity at the lesion site. As histologically seen, this activity is initially caused to an inflammatory cell response to the injury. Over time, this process involves the proliferation of healing cells, endosteal infiltration into the implant pores, neovascularization, and ultimately the formation of new bone (osteoconduction) and osteointegration. This results in a direct anchorage of the implant due to the formation of bony tissue not only around the implant but also throughout the main interconnected pores that are joined to the surrounding bone tissue, without any signs of fibrous tissue growth at the bone-implant interface.

CH, despite its weak properties, synergizes with HA enhance mechanical strength and osteogenicity. Grafting PP with polar monomers, such as monomethylitaconate, enhanced its interfacial adhesion to polar polymers such as CH with less toxicity than other grafting agents²⁸. Porous PP coated with CH and HA offers a chemical surface and topography favorable for a close implant bone interaction making a sculptable biocompatible implant material for low load-bearing applications.

We have concluded that when grafted PP is coated with CH and HA, and has a controlled pore size, it can be used as an implant under minimally loaded conditions. This allows the surrounding bone tissue to invade the pores of the implanted material, leading to proper osteointegration and osteoconduction resulting in what appears to be an anchored bone implant. The close interaction between the implant and the surrounding bone tissue, as described in this report, is highly desirable for biocompatible craniomaxillofacial reconstructive bone surgery.

Declaration of competing interest

The authors declare that they have no known competing financial interests or personal relationships that could have appeared to influence the work reported in this article.

Acknowledgements

Parts of this work were performed in Animal

Management Unit Facilities (UMA), Department of Clinical Science, Faculty of Veterinary and Animal Science, University of Chile, Santiago, Chile. The authors, gratefully acknowledge Dr. Dave Carrino, CWRU, for critically revising the manuscript.

References

- [1]. Das H. Bone Regeneration: Concepts, Clinical Aspects and Future Directions. Hauppauge, NY: Nova Sci. Publ.; 2018. p. 370.
- [2]. Duda GN, Geissler S, Checa S, Tsitsilonis S, Petersen A, Schmidt-Bleek K. The decisive early phase of bone regeneration. *Nat Rev Rheumatol*. 2023;19:78-95.
- [3]. Oliveira JM, Pina S, Reis RL, Roman JS. *Osteochondral Tissue Engineering*. Switzerland: Springer International Publishing AG; 2018.
- [4]. Pereira HF, Cengiz IF, Silva FS, Reis RL, Oliveira JM. Scaffolds and coatings for bone regeneration. *J Mater Sci Mater Med*. 2020;31:27.
- [5]. Wang W, Yeung KWK. Bone grafts and biomaterials substitutes for bone defect repair: A review. *Bioact Mater*. 2017;2:224-47.
- [6]. Kohn J, Welsh WJ, Knight D. A new approach to the rationale discovery of polymeric biomaterials. *Biomaterials*. 2007;28:4171-7.
- [7]. Reznikov N, Shahar R, Weiner S. Bone hierarchical structure in three dimensions. *Acta Biomater*. 2014;10:3815-26.
- [8]. Davies JE. Understanding peri-implant endosseous healing. *J Dent Educ*. 2003;67:932-49.
- [9]. Loi F, Córdova LA, Pajarinen J, Lin T, Yao Z, Goodman SB. Inflammation, fracture and bone repair. *Bone*. 2016;86:119-30.
- [10]. Marsell R, Einhorn TA. The biology of fracture healing. *Injury*. 2011;42:551-5.
- [11]. Daculsi G, Fella BH, Miramond T, Durand M. Osteoconduction, Osteogenicity, Osteoinduction, what are the fundamental properties for a smart bone substitutes. *IRBM*. 2013;34:346-8.
- [12]. Cortizo MS, Molinuevo MS, Cortizo AM. Biocompatibility and biodegradation of polyester and polyfumarate based-scaffolds for bone tissue engineering. *J Tissue Eng Regen Med*. 2008;2:33-42.
- [13]. Griffith LG. Polymeric biomaterials. *Acta Mater*. 2000;48:263-77.
- [14]. Li X, Feng Q, Jiao Y, Cui F. Collagen-based scaffolds reinforced by chitosan fibres for bone tissue engineering. *Polym Int*. 2005;54:1034-40.
- [15]. Al-allaq AA, Kashan JS, Abdul-Kareem FM. In vivo investigations of polymers in bone tissue engineering: a review study. *Int J Polym Mater Polym Biomater*. 2024. doi:10.1080/00914037.2024.2305227.

- [16]. Mata A, Geng Y, Henrikson KJ, Aparicio C, Stock SR, Satcher RL, et al. Bone regeneration mediated by biomimetic mineralization of a nanofiber matrix. *Biomaterials*. 2010;31:6004-12.
- [17]. Neunzehn J, Szuwart T, Wiesmann HP. Eggshells as natural calcium carbonate source in combination with hyaluronan as beneficial additives for bone graft materials, an in vitro study. *Head Face Med*. 2015;11:12.
- [18]. Durmuş E, Celik I, Ozturk A, Ozkan Y, Aydin M. Evaluation of the potential beneficial effects of ostrich eggshell combined with eggshell membranes in healing of cranial defects in rabbits. *J Int Med Res*. 2003;31:223-30.
- [19]. Zhang H, Wei Q, Ji R, Xie E, Sun A, Xiao B, et al. Biodegradable composites of poly(propylene carbonate) mixed with silicon nitride for osteogenic activity of adipose-derived stem cells and repair of bone defects. *J Mater Chem B*. 2023;11:6922-33.
- [20]. Fikai A, Andronescu E, Trandafir V, Ghitulica C, Voicu G. Collagen/hydroxyapatite composite obtained by electric field orientation. *Mater Lett*. 2010;64:541-4.
- [21]. Ardelean IL, Gudovan D, Fikai D, Fikai A, Andronescu E, Albu-Kaya MG, et al. Collagen/hydroxyapatite bone grafts manufactured by homogeneous/heterogeneous 3D printing. *Mater Lett*. 2018;231:179-82.
- [22]. Chatzipetros E, Christopoulos P, Donta C, Tosios KI, Tsiambas E, Tsiourvas D, et al. Application of nano-hydroxyapatite/chitosan scaffolds on rat calvarial critical-sized defects: A pilot study. *Med Oral Patol Oral Cir Bucal*. 2018;23:e625-e32.
- [23]. Arias JI, Neira-Carrillo A, Yazdani-Pedram M, Fernandez MS, Arias JL. A New Multilayered Composite Bioceramic for Bone Graft. In: Kisailus D, Estroff L, Gupta HS, Landis WJ, Zavattieri PD, editors. *Structure-Property Relationships in Biomineralized and Biomimetic Composites*. Vol 1187. 2009. p. 169-74.
- [24]. Biazar E, Heidari Keshel S, Tavirani MR, Jahandideh R. Bone reconstruction in rat calvarial defects by chitosan/hydroxyapatite nanoparticles scaffold loaded with unrestricted somatic stem cells. *Artif Cells Nanomed Biotechnol*. 2015;43:112-6.
- [25]. Khorasani M, Janbaz P, Rayati F. Maxillofacial reconstruction with Medpor porous polyethylene implant: A case series study. *J Korean Assoc Oral Maxillofac Surg*. 2018;44:128-35.
- [26]. Liao CZ, Li K, Wong HM, Tong WY, Yeung KWK, Tjong SC. Novel polypropylene biocomposites reinforced with carbon nanotubes and hydroxyapatite nanorods for bone replacements. *Mater Sci Eng C*. 2013;33:1380-8.
- [27]. López-Manchado MA, Kenny JM, Quijada R, Yazdani-Pedram M. Effect of grafted pp on the properties of thermoplastic elastomers based on pp-epdm blends. *Macromol Chem Phys*. 2001;202:1909-16.
- [28]. Neira-Carrillo A, Fernández MS, Arias JL, Navarrete G, Díaz MP, Yazdani-Pedram M. Preparation of a porous scaffold based on polypropylene grafted with monomethylitaconate as potential bone graft. *Macromol Res*. 2011;19:1105.
- [29]. De Lucca L, da Costa Marques M, Weinfeld I. Guided bone regeneration with polypropylene barrier in rabbit's calvaria: A preliminary experimental study. *Heliyon*. 2018;4:e00651.
- [30]. Bakker D, van Blitterswijk CA, Hesselting SC, Daems WT, Grote JJ. Tissue/biomaterial interface characteristics of four elastomers. A transmission electron microscopical study. *J Biomed Mater Res*. 1990;24:277-93.
- [31]. Bakker D, van Blitterswijk CA, Hesselting SC, Koerten HK, Kuijpers W, Grote JJ. Biocompatibility of a polyether urethane, polypropylene oxide, and a polyether polyester copolymer. A qualitative and quantitative study of three alloplastic tympanic membrane materials in the rat middle ear. *J Biomed Mater Res*. 1990;24:489-515.
- [32]. Bonner M, Ward IM, McGregor W, Tanner KE, Bonfield W. Hydroxyapatite/polypropylene composite: A novel bone substitute material. *J Mater Sci Lett*. 2001;20:2049-51.
- [33]. Liu Y, Wang M. Fabrication and characteristics of hydroxyapatite reinforced polypropylene as a bone analogue biomaterial. *J Appl Polym Sci*. 2007;106:2780-90.
- [34]. Zhao J, Han W, Chen H, Tu M, Huan S, Miao G, et al. Fabrication and in vivo osteogenesis of biomimetic poly(propylene carbonate) scaffold with nanofibrous chitosan network in macropores for bone tissue engineering. *J Mater Sci Mater Med*. 2012;23:517-25.
- [35]. Morais DS, Ávila B, Lopes C, Rodrigues MA, Vaz F, Machado AV, et al. Surface functionalization of polypropylene (PP) by chitosan immobilization to enhance human fibroblasts viability. *Polym Test*. 2020;86:106507.
- [36]. Liu T, Huang K, Li L, Gu Z, Liu X, Peng X, et al. High performance high-density polyethylene/hydroxyapatite nanocomposites for load-bearing bone substitute: fabrication, in vitro and in vivo biocompatibility evaluation. *Compos Sci Technol*. 2019;175:100-10.
- [37]. Morse A. Formic Acid-Sodium Citrate Decalcification and Butyl Alcohol Dehydration of Teeth and Bones for Sectioning in Paraffin. *J Dent Res*. 1945;24:143-53.
- [38]. Orhan ZD, Ciğerim L. Evaluation of the Effect of Polybutester and Polypropylene Sutures on Complications after Impacted Lower Third Molar Surgery. *Appl Sci*. 2024;14:1448.
- [39]. Bahhtiari H, Nouri A, Khakbiz M, Tolouei-Rad M. Fatigue behaviour of load-bearing polymeric bone scaffolds: A review. *Acta Biomater*. 2023;172:16-37.

- [40].Castro F, Bouzidi AS, Fernandes JCH, Bottino MC, Fernandes GVO. Bone tissue regeneration in peri-implantitis: A systematic review of randomized clinical trials. *Saudi Dent J*. 2023.
- [41].Karageorgiou, V. & Kaplan, D. (2005) 'Porosity of 3D biomaterial scaffolds and osteogenesis', *Biomaterials*, 26(27), pp. 5474-5491
- [42].Neira-Carrillo, A., Fernández, M. S., Arias, J. L., Navarrete, S., Díaz, M. P. & Yazdani-Pedram, M. (2011) 'Preparation of a porous scaffold based on polypropylene grafted with monomethylitaconate as potential bone graft', *Macromolecular Research*, 19(11), pp. 1105-1113.
- [43].Lee JE, Kim SE, Kwon IC, Ahn HJ, Cho H, Lee SH, Kim HJ, Seong SC, Lee MC. Effects of a chitosan scaffold containing TGF-beta1 encapsulated chitosan microspheres on in vitro chondrocyte culture. *Artif Organs*. 2004;28:829-39.
- [44].Seol YJ, Lee JY, Park YJ, Lee YM, Young-Ku, Rhyu IC, et al. Chitosan sponges as tissue engineering scaffolds for bone formation. *Biotechnol Lett*. 2004;26:1037-41.
- [45].Arpornmaeklong P, Suwatwirote N, Pripatnanont P, Oungbho K. Growth and differentiation of mouse osteoblasts on chitosan-collagen sponge. *Int J Oral Maxillofac Surg*. 2007;36:328-37.
- [46].Sheehy EJ, Mesallati T, Vinardell T, Kelly DJ. Engineering cartilage or endochondral bone: A comparison of different naturally derived hydrogels. *Acta Biomater*. 2015;13:245-53.
- [47].Elieh-Ali-Komi D, Hamblin MR. Chitin and chitosan: production and application of versatile biomedical nanomaterials. *Int J Adv Res (Indore)*. 2016;4:411-27.
- [48].Muzzarelli RA, Mattioli-Belmonte M, Tietz C, Biagini R, Ferioli G, Brunelli MA, et al. Stimulatory effect on bone formation exerted by a modified chitosan. *Biomaterials*. 1994;15:1075-81.
- [49].Shin Y, Yoo DI, Min K. Water-soluble chitosan oligomer was prepared for finishing polypropylene nonwoven fabrics to impart antimicrobial activity. *J Appl Polym Sci*. 1999;74:2911-6.
- [50].Peniche C, Solís Y, Davidenko N, García R. Chitosan/hydroxyapatite-based composites. *Biotechnol Appl*. 2010;27:202-10.
- [51].Li H, Zhou C, Zhu M, Tian J, Rong J. Preparation and characterization of homogeneous hydroxyapatite/chitosan composite scaffolds via in-situ hydration. *J Biomater Nanobiotechnol*. 2010;1:42-9.
- [52].Oliveira JM, Rodrigues MT, Silva SS, Malafaya PB, Gomes ME, Viegas CA, et al. Novel hydroxyapatite/chitosan bilayered scaffold for osteochondral tissue-engineering applications: Scaffold design and its performance when seeded with goat bone marrow stromal cells. *Biomaterials*. 2006;27:6123-37.
- [53].Bushra A, Subhani A, Islam N. A comprehensive review on biological and environmental applications of chitosan-hydroxyapatite biocomposites. *Compos Part C Open Access*. 2023;12:100016.
- [54].Kashirina A, Yao Y, Liu Y, Leng J. Biopolymers as bone substitutes: a review. *Biomater Sci*. 2019;7:3961-83.
- [55].Sheikh Z, Najeeb S, Khurshid Z, Verma V, Rashid H, Glogauer M. Biodegradable materials for bone repair and tissue engineering applications. *Materials (Basel)*. 2015;8:5744-53.
- [56].Paxton NC, Allenby MC, Lewis PM, Woodruff MA. Biomedical applications of polyethylene. *Eur Polym J*. 2019;118:412-28.
- [57].Bronner F, Farach-Carson MC, Mikos AG. Engineering of functional skeletal tissues. London: Springer; 2007. p. xii, 178 p.
- [58].Galois L, Mainard D, Delagoutte JP. Bone ingrowth into two porous ceramics with different pore sizes: An experimental study. *Acta Orthop Belg*. 2002;68(1):30-5.
- [59].Bai X, Gao M, Syed S, Zhuang J, Xu X. Bioactive hydrogels for bone regeneration. *Bioact Mater*. 2018;3:401-17.
- [60].Murphy CM, Haugh MG, O'Brien FJ. The effect of mean pore size on cell attachment, proliferation, and migration in collagen-glycosaminoglycan scaffolds for tissue engineering. *Biomaterials*. 2010;31:461-6.
- [61].Landry PS, Marino AA, Sadasivan KIK, Albright JA. Bone injury response. An animal model for testing theories of regulation. *Clin Orthop Relat Res*. 1996;332:260-73.